# Thermoresponsiveness of Integrated Ultra-Thin Silicon with Poly(*N*-isopropylacrylamide) Hydrogels[a]

Cunjiang Yu, Yuping Pan, Huan Ma, Teng Ma, Jiaping Zhang, Yanmei Song, M. Yashar S. Kalani, Lenore Dai, Hanqing Jiang*

Stimuli-sensitive polymer materials have limited device functionality, design and manufacturing flexibility although they are pushed to enable smart device applications. Here we demonstrate the capability of integrating thermoresponsive poly(*N*-isopropylacrylamide) (PNIPAAm) hydrogels with silicon nanoribbons, and enable the stiff silicon ribbons to become adaptive and drivable by the soft environmentally sensitive substrate, such as becoming mechanically stretched and compressed on temperature change. These and related soft/hard smart devices and systems may open new opportunities in biomedical applications.
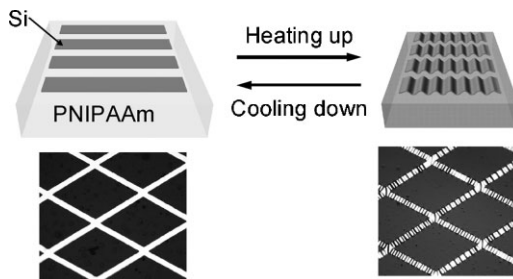
Introduction

The development of next-generation smart and intelligent devices that autonomously transduce environmental signals has emerged as one of the most interesting areas of material science. The materials for such devices mostly involve polymers that are sensitive and able to respond to a variety of stimuli, including light, pH, temperature, humidity, as well as electrical fields.[1–7] They primarily show dynamic structural or mechanical responses upon changes to their ambient environment. Hydrogel, one of the most prominent examples of such responsive polymers, is able to swell and shrink in solvents (e.g., water) and has found many successful applications such as in microfluidics,[8–14] actuators,[15–18] artificial muscles,[19–22] and precise micro/nano-manipulation.[23–25] The commonly investigated adaptive hydrogels, however, naturally offer limited functionality or design flexibility for adaptive device applications, compared with many other functional semiconductor materials (e.g., Si). Therefore, the development of environmentally sensitive electronics requires one to explore the feasibility of the combination of adaptive materials and functional components.

Another demand for environmentally sensitive electronics is their low mechanical stiffness and high flexibility to adapt to the presence of complicated boundary constraints, such as mounting with rough surfaces. Recently, thin films of crystal semiconductors (e.g., Si) have shown potential application for flexible and stretchable electronics when they are integrated with elastomeric substrates (e.g., poly(dimethylsiloxane) (PDMS)). Using this technology, diodes, transistors, logic gate circuits, and more complex devices such as curvy electronic eyes have been demonstrated.[5,26–30] Specifically, these devices combine the merits of high quality crystalline semiconductor materials and the mechanical flexibility/stretchability of elastomers, although the environmental sensitivity has not yet been

C. Yu, Y. Pan, H. Ma, T. Ma, J. Zhang, Y. Song, Prof. L. Dai, Prof. H. Jiang
School for Engineering of Matter, Transport and Energy, Arizona State University, Tempe, AZ 85287, USA
E-mail: hanqing.jiang@asu.edu
Dr. M. Yashar S. Kalani
Division of Neurological Surgery, Barrow Neurological Institute, St. Joseph's Hospital and Medical Center, Phoenix, AZ 85003, USA

realized. The combination of environmental responsiveness and mechanical flexibility/stretchability brings broader and more fascinating applications, such as electronic eyes with stimuli tunable curvatures that may be applied to the field of medical endoscopy, in the form of flexible, light sensitive endoscopes that can be used to maneuver into and visualize lesions in hard to reach spaces such as the cavernous sinus in the brain and the knee for arthroscopic applications.[31,32]

We report here an alternative approach to making thermoresponsive ultra-thin silicon nanostructures, in which several hundred nanometers thick silicon nanoribbons are integrated with hydrogels and are able to change their mechanical configurations rapidly upon altering the ambient temperature. Ultra-thin silicon ribbons become adaptive and can be reversibly driven to be flat and 'wavy' according to the cyclic change of the temperature. Figure 1a schematically shows the cyclic behavior of the silicon nanoribbons on thermally sensitive hydrogels. The integrated hydrogels (representing the environmentally sensitive materials) and silicon (a type of widely used functional material) presented here, represent a new class of combination between soft and hard materials, and opens ways for future environmentally sensitive electronics.
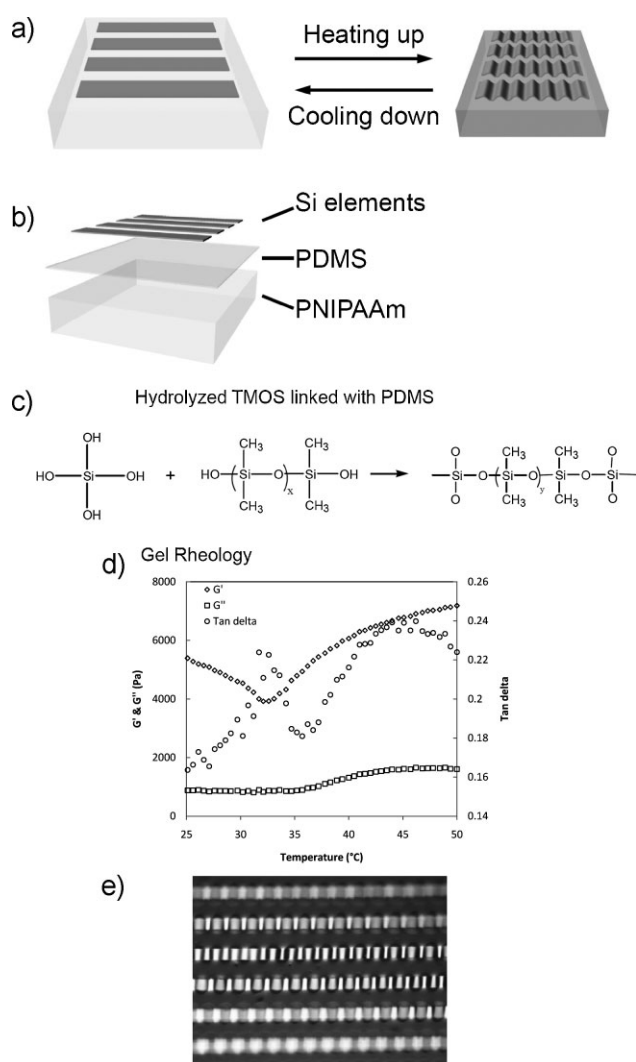
Experimental Section

Poly(N-isopropylacrylamide) (PNIPAAm) was chosen because of its large swelling ratio and sharp phase transition that have been extensively reported elsewhere.[1] The system consisted of three components, a PNIPAAm gel, a PDMS layer (which was vital for the latter high-yield transfer steps), and Si nanoribbons (Figure 1b). The synthesis of the PNIPAAm gel has been reported elsewhere.[33,34] In order to promote the bonding between the PNIPAAm gel and the PDMS layer, tetramethoxysilane (TMOS) was incorporated into the gel synthesis (see Supporting Information). Specifically, the silica network produced by hydrolyzed TMOS and N-isopropylacrylamide (NIPAAm) monomer during gel synthesis had residual Si–OH groups. The residual Si–OH groups attached to the silica network distributed inside the PNIPAAm gel network from TMOS, bonded with the hydroxy-terminated PDMS through a condensation reaction (Figure 1c).[33,34]

After the gel was synthesized and reached the equilibrium swollen state, a mixture of Sylgard 184 silicone elastomer (Dow Corning) base and curing agent (at the ratio of 30 : 1) was spread on the top surface of the swollen hydrogel slab. The uncured PDMS spontaneously spread out and formed a continuous thin layer with a smooth surface in a few minutes due to the flow driven by surface tension. Keeping the bottom gel swollen in water, the top PDMS layer was cured in air for several days at room temperature, allowing the PDMS to solidify. The thickness of the PDMS was measured by an optical microscope by cutting the PDMS/gel sample along the direction of the cross-section. The sample was exposed to ultraviolet light with atomic oxygen (UVO) for 150 s to generate hydroxy groups on the top surface of the PDMS layer, which was essential for transfer printing of Si thin films. The Si nanoribbons (50 μm wide, 5 000 μm long, and 100 nm thick) were fabricated using an established process (see Supporting Information),[27,35] and then transferred to the PNIPAAm hydrogel/UVO-treated PDMS system using a PDMS stamp. The PDMS stamp with Si nanoribbons was slightly brought into contact with the –OH rich surface of the UVO-treated PDMS and then slowly peeled off to prevent damaging the Si nanoribbons bonded to the UVO-treated PDMS. Efficient transfer was achieved since the interfacial chemical bonding between the Si/UVO-treated PDMS was much stronger than the physical adhesion between the PDMS stamp/Si interface.[27,30]

Figure 1. a) Schematic of the hydrogel swelling/shrinking drivable silicon thin ribbons. b) Layer-assembled structure. c) Formation of hydrolyzed TMOS linked with PDMS. d) Rheology testing of the synthesized hydrogel reveals a transition temperature around 33 °C. e) An optical image clearly showing out-of-plane buckling of thin Si nanoribbons on the PDMS/hydrogel when immersed in hot water.

Results and Discussion

The synthesized hydrogel was examined for a transition temperature, which represents one of the essential characteristics for the response of the devices upon temperature change (see Supporting Information). The rheology testing reveals that the transition temperature (defined as the peak of the tan delta) for the synthesized hydrogel is around 33 °C (Figure 1d). The storage modulus G' is much greater than the loss modulus G'' over the entire temperature range, suggesting that the hydrogel behaves more like a solid. G' increases rapidly right after the volume phase transition temperature, which indicates that the hydrogel becomes harder because of deswelling above 33 °C. The mechanism of the temperature responsiveness is as follows: As the ambient temperature is above the transition temperature, the hydrogel network becomes hydrophobic thus expels water and shrinks, which is a typical local critical solution temperature (LCST) phenomenon. For this sample, the dimension changes from 12 mm to 10 mm, i.e., a 16.7% linear strain or, equivalently, a 42% volumetric change, when the ambient temperature exceeds the transition temperature.

We expect that the constraint from the thin Si layers (100 nm thick) and soft/thin PDMS (0.2 MPa modulus and about 500 µm thick) is insufficient to influence or prevent the dimensional change of the hydrogel upon temperature variation. The 100 nm thick Si nanoribbons are initially transferred and printed onto flat, fully swollen hydrogel/PDMS surfaces at room temperature. When the transition temperature (here 33 °C) is reached, the PNIPAAm hydrogel shrinks and buckles the initially flat Si nanoribbons into periodic sinusoidal shapes. The out-of-plane buckling of the Si ribbons results from the compression load on the stiff/soft materials, where soft materials can undergo shrinking while stiff materials have to buckle to release the compressive strain, which has been reported elsewhere.[27,36–40] Figure 1e shows the optical image of a tilted view of the buckled Si nanoribbons on the mediate PDMS layer when immersed in 45 °C water. The buckling wavelength is around 29 µm. We notice that the Si buckling patterns are one-dimensional although the deswelling of PNIPAAm is two dimensional and isotropic. The explanation is that the

width of the Si nanoribbons, 50 µm, is comparable to the buckling wavelength (29 µm), thus two-dimensional buckling patterns (such as herringbone) would not appear for such narrow ribbons but are expected to be present when the ribbon width is much greater than the buckling wavelength.

We studied the evolution of the Si buckling patterns upon temperature change. The temperature change is realized by varying the ambient temperature of the solvent. Figure 2a provides a series of optical images showing the evolution of the buckling morphology of the Si nanoribbons. During the experiments, the hydrogel/PDMS/Si system was immersed into hot water in a Petri dish, allowing it to be heated and cooled. Image (i) shows the flat Si nanoribbon arrays bonded with the hydrogel/PDMS after transfer printing. Image (ii) shows the morphology of the hydrogel/PDMS/Si system after immersing in 45 °C water for 2 min, in which the buckling patterns appear. We actually observed that the
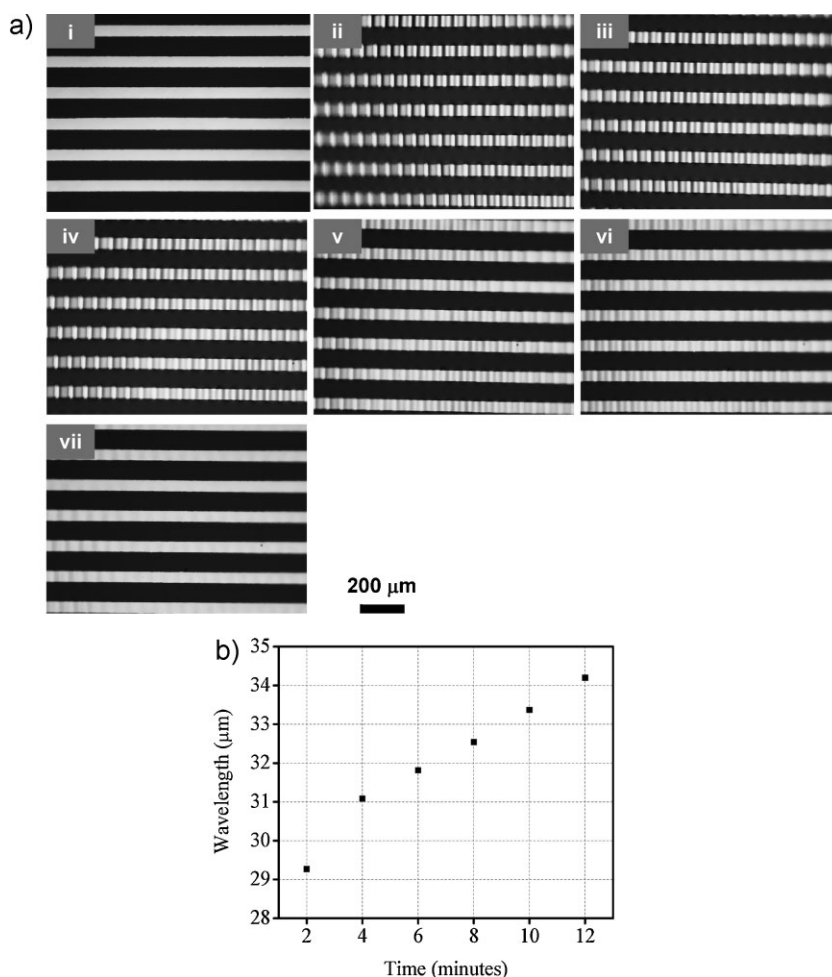

Figure 2. a) Buckling morphology evolution of the silicon thin ribbons. i) After transfer printing, ii) 2 min after immersion into hot water (45 °C), iii) 4 min, iv) 6 min, v) 8 min, vi) 10 min, and vii) 12 min. b) The wavelength of (ii) to (vii) in (a) increases during cooling of the ambient temperature while the hydrogel substrate swells.

822

*Macromolecular
Journals*

Macromol. Rapid Commun. **2011**, *32*, 820–824
© 2011 WILEY-VCH Verlag GmbH & Co. KGaA, Weinheim

*Materials
Views*

www.MaterialsViews.com

buckling patterns became obvious once the hydrogel/PDMS/Si system was immersed in 45 °C water for less than 10 s. This fast response (< 10 s) depends on various factors, including the monomers' temperature sensitivity, the structure of the gel, and more importantly the dimension of the PNIPPAm hydrogel slab because both the heat and mass transfer are related to the size of the media. Specifically, both heat conduction and mass diffusion timescales are of the order of L^2/k and L^2/D, where L is the characteristic length of the media, and k and D are thermal conductivity and mass diffusivity, respectively. Therefore, by decreasing the size of the hydrogel slab, the responsiveness timescale can be significantly reduced. However, there also exists a constraint that the hydrogel slab must be large enough to store sufficient elastic energy from the swelling/shrinking to drive the deformation of the PDMS/Si nanoribbons. Therefore, an optimum hydrogel dimension exists, which should be studied further.

Images (iii–vii) show the evolution of the buckling patterns at 4, 6, 8, 10, and 12 min, respectively. With time, the ambient temperature drops from 45 °C to room temperature, thus the hydrogel network becomes hydrophilic again and swells, which fades out the wrinkle patterns. Figure 2b shows that with time, the buckling wavelength (read from Figure 2a) monotonically increases in an almost linear fashion, which indicates the linear dimension change of the hydrogel as a result of cooling. The observed bucking shape evolution obeys the mechanics of finite deformation of non-linear buckled stiff thin films on compliant substrates.[40] When the temperature reaches room temperature, the hydrogel becomes fully swollen again and the buckling disappears driven by the temperature change. We also conducted cyclic heating and cooling experiments and found a very reliable repeatability of such thermoresponsiveness of the hydrogel/PDMS/Si nanoribbon systems.

The buckling of the Si/PDMS/gel system is qualitatively simulated using a commercial finite element analysis package, ABAQUS, to verify that the shrinking of the hydrogels is able to buckle nanometer-scale thin films. The finite element model consists of a 100 nm thick Si thin film and a 500 μm thick PDMS layer which are modeled as elastic materials, and a 500 μm thick gel layer. The three layers have the same length, 500 μm. The elastic modulus (E) and Poisson's ratio (ν) for Si and PDMS are $E_{Si} = 130$ GPa, $\nu_{Si} = 0.3$,[41] and $E_{PDMS} = 0.2$ MPa, $\nu_{PDMS} = 0.49$, respectively. The gel is modeled by a Flory and Rehner[42] model that has been recently used to develop a field theory with coupled large deformation and diffusion.[43,44] The shear modulus of the dry PNIPAAm gel is measured by a dynamic mechanical analyzer as 40 MPa. The temperature sensitivity of the PNIPAAm gel is characterized by Flory's dimensionless parameter χ which describes the hydrophilicity of the polymer. Specifically, χ changes from 0.09 to 0.46 to describe
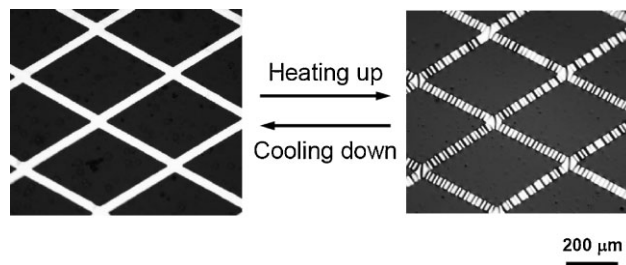

Figure 3. Demonstration of the thin Si diamond network structure becoming buckled when the hydrogel substrate shrinks.

the shrinking of a gel from a swelling ratio of 1.2 to 1.15, i.e., a 4% compressive strain is applied to the Si/PDMS/gel system. The finite element analysis obtains a buckling wavelength of 36.6 μm. It is noticed that the strain used in the finite element simulation (4%) is smaller than that in the experiments (16.7%), which qualitatively explains the discrepancy in wavelength between modeling and experiments. However, the most important message has been verified by numerical simulations, i.e., the shrinking of the gels can buckle hard materials with nanometer thickness.

In addition to the aforementioned one-dimensional Si nanoribbons, ultra-thin Si-based network structures were integrated with hydrogels and their thermoresponsiveness has also been demonstrated. Following the same experimental procedure for the Si nanoribbons, a diamond-shaped Si network structure of 100 nm thickness and 400 μm in length for each side becomes buckled when the hydrogel shrinks upon exceeding the transition temperature (Figure 3). The diamond-shaped network retains its shape during the dynamic buckling and recovery process because of the isotropic swelling and shrinking of the PNIPAAm hydrogel.

Conclusion

In summary, we have validated thermoresponsive ultra-thin Si driven by hydrogels. When the transition temperature of the hydrogel is reached, the swelling or shrinkage of the hydrogel drives the deformation of the Si elements by means of generating buckling patterns. Integration of such a new class of environmentally sensitive hydrogels with functional electronics materials provides important capabilities for the development of inorganic environmentally sensitive electronics. Areas for future work include various stimuli responsive inorganic functional devices and autonomous adaptive biomedical systems such as electronic eyes with environmentally tunable focuses.

[1] E. S. Gil, S. M. Hudson, *Prog. Polym. Sci.* **2004**, *29*, 1173.

[2] A. Lendlein, H. Y. Jiang, O. Junger, R. Langer, *Nature* **2005**, *434*, 879.

[3] Y. Osada, H. Okuzaki, H. Hori, *Nature* **1992**, *355*, 242.

[4] J. Lahann, S. Mitragotri, T. N. Tran, H. Kaido, J. Sundaram, I. S. Choi, S. Hoffer, G. A. Somorjai, R. Langer, *Science* **2003**, *299*, 371.

[5] A. Richter, G. Paschew, S. Klatt, J. Lienig, K. F. Arndt, H. J. P. Adler, *Sensors* **2008**, *8*, 561.

[6] E. T. Tian, J. X. Wang, Y. M. Zheng, Y. L. Song, L. Jiang, D. B. Zhu, *J. Mater. Chem.* **2008**, *18*, 1116.

[7] F. J. Arregui, Z. Ciaurriz, M. Oneca, I. R. Matias, *Sens. Actuators B* **2003**, *96*, 165.

[8] D. J. Beebe, J. S. Moore, J. M. Bauer, Q. Yu, R. H. Liu, C. Devadoss, B. H. Jo, *Nature* **2000**, *404*, 588.

[9] D. T. Eddington, D. J. Beebe, *J. Microelectromech. Syst.* **2004**, *13*, 586.

[10] S. H. Lee, D. T. Eddington, Y. M. Kim, W. S. Kim, D. J. Beebe, *J. Microelectromech. Syst.* **2003**, *12*, 848.

[11] A. K. Agarwal, S. S. Sridharamurthy, D. J. Beebe, H. R. Jiang, *J. Microelectromech. Syst.* **2005**, *14*, 1409.

[12] L. Dong, A. K. Agarwal, D. J. Beebe, H. R. Jiang, *Nature* **2006**, *442*, 551.

[13] M. Lei, Y. D. Gu, A. Baldi, R. A. Siegel, B. Ziaie, *Langmuir* **2004**, *20*, 8947.

[14] A. Richter, S. Klatt, G. Paschew, C. Klenke, *Lab Chip* **2009**, *9*, 613.

[15] A. Sidorenko, T. Krupenkin, A. Taylor, P. Fratzl, J. Aizenberg, *Science* **2007**, *315*, 487.

[16] M. Bassil, J. Davenas, M. El Tahchi, *Sens. Actuators B* **2008**, *134*, 496.

[17] Y. K. Yew, T. Y. Ng, H. Li, K. Y. Lam, *Biomed. Microdevices* **2007**, *9*, 487.

[18] Y. Zhang, S. Kato, T. Anazawa, *Smart Mater. Struct.* **2007**, *16*, 2175.

[19] Z. S. Liu, P. Calvert, *Adv. Mater.* **2000**, *12*, 288.

[20] L. J. Mao, Y. J. Hu, Y. S. Piao, X. D. Chen, W. S. Xian, D. X. Piao, *Curr. Appl. Phys.* **2005**, *5*, 426.

[21] E. A. Moschou, M. J. Madou, L. G. Bachas, S. Daunert, *Sens. Actuators B* **2006**, *115*, 379.

[22] E. A. Moschou, S. F. Peteu, L. G. Bachas, M. J. Madou, S. Daunert, *Chem. Mater.* **2004**, *16*, 2499.

[23] J. H. Kang, J. H. Moon, S. K. Lee, S. G. Park, S. G. Jang, S. Yang, S. M. Yang, *Adv. Mater.* **2008**, *20*, 3061.

[24] B. Kaehr, J. B. Shear, *Proc. Natl. Acad. Sci. USA* **2008**, *105*, 8850.

[25] J. Kim, J. Yoon, R. C. Hayward, *Nat. Mater.* **2010**, *9*, 159.

[26] W. M. Choi, J. Z. Song, D. Y. Khang, H. Q. Jiang, Y. Y. Huang, J. A. Rogers, *Nano Lett.* **2007**, *7*, 1655.

[27] D. Y. Khang, H. Q. Jiang, Y. Huang, J. A. Rogers, *Science* **2006**, *311*, 208.

[28] D. H. Kim, J. H. Ahn, W. M. Choi, H. S. Kim, T. H. Kim, J. Z. Song, Y. G. Y. Huang, Z. J. Liu, C. Lu, J. A. Rogers, *Science* **2008**, *320*, 507.

[29] H. C. Ko, M. P. Stoykovich, J. Z. Song, V. Malyarchuk, W. M. Choi, C. J. Yu, J. B. Geddes, J. L. Xiao, S. D. Wang, Y. G. Huang, J. A. Rogers, *Nature* **2008**, *454*, 748.

[30] Y. G. Sun, W. M. Choi, H. Q. Jiang, Y. G. Y. Huang, J. A. Rogers, *Nat. Nanotechnol.* **2006**, *1*, 201.

[31] B. Abuzayed, N. Tanriover, N. Gazioglu, Z. Akar, *J. Craniofac. Surg.* **2010**, *21*, 245.

[32] P. G. Campbell, E. Kenning, D. W. Andrews, S. Yadla, M. Rosen, J. J. Evans, *Neurosurgical Focus* **2010**, *29*, E5.

[33] B. Strachotova, A. Strachota, M. Uchman, M. Slouf, J. Brus, J. Plestil, L. Matejka, *Polymer* **2007**, *48*, 1471.

[34] G. D. Kim, D. A. Lee, J. W. Moon, J. D. Kim, J. A. Park, *Appl. Organomet. Chem.* **1999**, *13*, 361.

[35] C. J. Yu, Z. Y. Wang, H. Y. Yu, H. Q. Jiang, *Appl. Phys. Lett.* **2009**, 95.

[36] N. Bowden, S. Brittain, A. G. Evans, J. W. Hutchinson, G. M. Whitesides, *Nature* **1998**, *393*, 146.

[37] N. Bowden, W. T. Huck, K. E. Paul, G. M. Whitesides, *Appl. Phys. Lett.* **1999**, *75*, 2557.

[38] K. Efimenko, M. Rackaitis, E. Manias, A. Vaziri, L. Mahadevan, J. Genzer, *Nat. Mater.* **2005**, *4*, 293.

[39] J. Genzer, J. Groenwold, *Soft Matter* **2006**, *2*, 310.

[40] H. Jiang, D. Y. Khang, J. Song, Y. Sun, Y. Huang, J. A. Rogers, *Proc. Natl. Acad. Sci. USA* **2007**, *104*, 15607.

[41] INSPEC, ''Properties of Silicon'', Institution of Electrical Engineers, New York **1988**.

[42] P. J. Flory, J. Rehner, *J. Chem. Phys.* **1943**, *11*, 521.

[43] W. Hong, X. H. Zhao, J. X. Zhou, Z. G. Suo, *J. Mech. Phys. Solids* **2008**, *56*, 1779.

[44] J. P. Zhang, X. H. Zhao, Z. G. Suo, H. Q. Jiang, *J. Appl. Phys.* **2009**, *105*, 9.